JOURNAL OF GEOPHYSICAL RESEARCH, VOL. 96, NO. B3, PAGES 4065–4082, MARCH 10, 1991

Paleomagnetic Study of Mesozoic Continental Sediments Along the Northern Tien Shan (China) and Heterogeneous Strain in Central Asia

YAN CHEN,[1] JEAN-PASCAL COGNE,[1,2] VINCENT COURTILLOT,[1] JEAN-PHILIPPE AVOUAC,[1] PAUL TAPPONNIER,[1] GONGQUE WANG,[4] MEIXIANG BAI,[5] HONGZI YOU,[4] MING LI [4] AND CHUNSHENG WEI [4] ERIC BUFFETAUT.[3]

A paleomagnetic study of rocks from the northern foot of the Tien Shan and the southern border of the Dzungar Basin, east of Urumqi (44.2°N, 86.0°E), spanning ages from middle Jurassic to early Tertiary was carried out to constrain the tectonic evolution in central Asia since Mesozoic time. Five middle Jurassic sites reveal a remagnetized direction close to the present Earth field in geographic coordinates: $D = 6.6°$, $I = 72.6°$ ($\alpha_{95} = 7.4°$). Thirteen out of 17 upper Jurassic and lower Cretaceous sites yield a characteristic direction (stratigraphic coordinates) of $D = 12.7°$, $I = 48.6°$ ($\alpha_{95} = 5.5°$). Nine of 16 upper Cretaceous and lower Tertiary sites provide a characteristic direction of $D = 12.5°$, $I = 51.3°$ ($\alpha_{95} = 6.9°$). The latter two directions pass fold and reversal tests. The pole positions are close to each other and to the Besse and Courtillot [1989, 1990] Eurasian apparent polar wander path, for ages ranging from 130 to 70 Ma. However, the difference in paleolatitudes amounts to about 5.9° ± 3.7°, which could indicate significant continental shortening in the Altai Mountains and perhaps further north, subsequent to India-Asia collision. The pole positions from the Dzungar Basin are close to those found for the Tarim [Li et al., 1988a], leading to an insignificant paleolatitude difference (3.0° ± 6.9°), but showing a larger difference in declination (8.6° ± 8.7°). These paleomagnetic results are compatible with a model of heterogeneous deformation in the western part of the collision zone between India and Siberia. A significant shortening in the Altai, a slight counterclockwise rotation of the Dzungar block, the westward-increasing shortening in the Tien Shan with attendant clockwise rotation of the Tarim block are all consistent with this model, in which Tibet, the Tien Shan and the Altai undergo differential strain along strike in a relay fashion, with the total India-Siberia convergence remaining approximately constant.

Introduction

Central Asia consists of a mosaic of blocks which accreted since the early Paleozoic. Based mostly on paleontology and stratigraphy, and on the recognition of tectonic boundaries, a number of blocks with different geological histories have now been identified: Siberia, Tarim, Kazakhstan, North China, South China, Indochina, and the Tibetan blocks. However, the timing of individual collisions is still debated, sometimes hotly so. For instance, *Li et al.* [1982] propose that the North and South China blocks were accreted in the Triassic, whereas *Laveine et al.* [1987] and *Mattauer et al.* [1985] propose a Paleozoic age.

Paleomagnetism provides an independent source of data bearing on this problem. *Opdyke et al.* [1986] use such data to favor a post-Triassic age of North versus South China collision. *McElhinny et al.* [1981] and *Li et al.* [1988b] believe that Tarim and North China behaved as independent units in the Permian, whereas *Li* [1980] finds no evidence for a suture between the two.

A significant amount of paleomagnetic research has recently been published or is underway in central and eastern Asia. Data have been collected from Tibet [*Achache et al.*, 1984], South China [e.g., *Kent et al.*, 1986; *Enkin et al.*, 1991*a*, *b*), and farther north from North China [e.g.,*Lin*, 1984] and the Tarim [e.g., *Li et al.*, 1988*a*, *b*]. This leaves the important Dzungar block relatively unexplored. With a surface area of 130,000 km^2, this large basin has traditionally been considered a part of the Kazakhstan, wedged between the Tarim and Siberia blocks (Figures 1 and 16). Its boundary with the former lies along the Tien Shan range and with the latter along the Altai range, where ophiolite suites and ophiolite mélanges have been found [*Li et al.*, 1982; *Zhang and Wu*, 1985].

In recent years, research carried out in the Gansu corridor between Tarim and North China, and in the Tarim and Dzungar basins has focused primarily on Permian and Triassic formations [*Bai et al.*, 1987; *Li*, 1988; *Li et al.*, 1989]. Yet the configuration of the Eurasian mosaic has been profoundly altered by the India-Asia collision [*Molnar and Tapponnier*, 1975; *Tapponnier and Molnar*, 1979; *Tapponnier et al.*, 1986]. The first results from the French-Chinese paleomagnetic work in Tibet suggested some 2000 km of shortening between Tibet and Siberia [*Achache et al.*, 1984] and total shortening could be even larger, based on revisions of the apparent polar wander path of Eurasia [*Besse and Courtillot*, 1991] and on the age of the onset of collision [*Jaeger et al.*, 1989].

It is therefore important to reconstruct the precollisional paleogeography of Asia and to determine in a quantitative fashion the amount of subsequent intracontinental

[1] Institut de Physique du Globe de Paris and Département des Sciences de la terre, Université Paris VII.
[2] CAESS, Université Rennes I
[3] Centre National de la Recherche Scientifique, Laboratoire de Paléontologie des Vertébrés, Université Paris VI.
[4] Xinjiang Engineering Institute, People's Republic of China.
[5] Bureau of seismology of Xinjiang, People's Republic of China.

Paper number 90JB02699.
0148-0227/91/90JB-02699$05.00

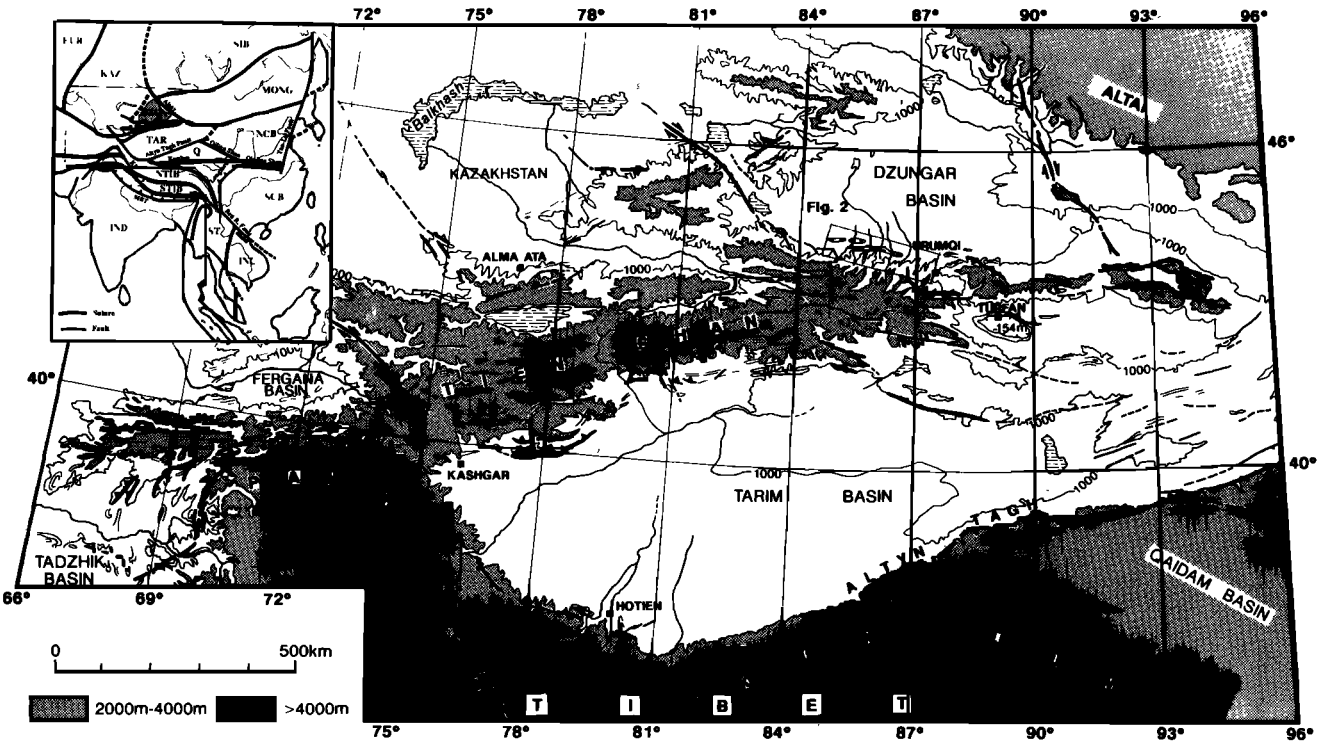

Fig. 1. Topographic map of Central Asia showing main basins (Tarim and Dzungar) and ranges (Tibet, Pamir, Tien Shan and Altai); contours every 1000 m. The box near Urumqi corresponds to the studied area (Figure 2) [after *Tapponnier and Molnar*, 1979; *J.P. Avouac et al.*, manuscript in preparation, 1991]. The inset is a sketch map of the main tectonic units (see also Figure 16).

deformation. This requires collection of Mesozoic and Cenozoic formations, which have apparently been less studied, particularly in the Dzungar block. This paper reports the first results of a paleomagnetic sampling in the region west of Urumqi and north of the foot of the Tien Shan Mountains (44.2°N, 86.0°E), along the southern edge of the Dzungar basin (Figure 2).

GEOLOGY AND SAMPLING

The well-exposed rock sequences generally consist of soft, coarse-grained continental sediments. Some harder strata were found to be better suited for paleomagnetic sampling. Drill cores (445) were taken from 38 sites in rocks dating from the middle Jurassic to the early Tertiary. Dating the continental

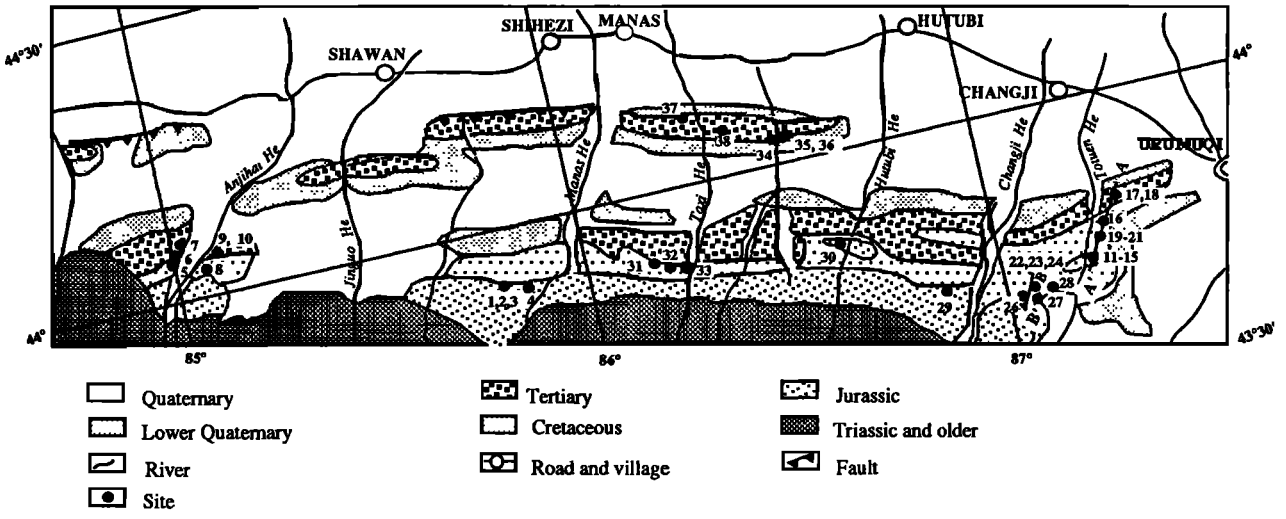

Fig. 2. Schematic geological map of sampling area, including site locations (solid circles). Cross sections AA' and BB' are shown in Figure 3.

rocks of the Dzungar basin with some accuracy is difficult because of the scarcity of fossils. Thus we divided our paleomagnetic sampling into three age sequences: middle Jurassic, late Jurassic-early Cretaceous and late Cretaceous-early Tertiary. The sites are distributed along a 120-km-long stretch west of Urumqi (Table 1 and Figure 2).

Middle Jurassic Totuenhe Formation (J_{2t})

This sequence of dark-red and green-grey medium-grained sandstone is more than 500 m thick. It is monoclinal with near vertical dips (even overturned, Figure 3) and contains fossil plants such as *Ginkgoites sibericus*, *Baieria cf. gracilis* and *Pterophyllum sp.* (Bureau of Petroleum Geology of Xinjiang, personal communication, 1988). According to *Wang* [1985], this formation is Bathonian to Callovian in age. Ostracodes reported from this formation, such as *Timiriasevia catenularia Mandelstam* and *Darwinula impudica Sharapova* also suggest a Middle Jurassic age (J. F. Babinot, personal communication, 1989). From this sequence we collected a total of 60 samples in five sites in deep-red strata along the east side of the Totuenhe River (Table 1 and Figure 2).

Late Jurassic Qigou (J_{3q})-Early Cretaceous Hutubi (K_{1h}) Formations

These formations make up a total of more than 1000 m of sediments. The rocks consist of beds of coarse to medium-grained sandstones, some of them dark red, others grey-green.

TABLE 1. Site Data

Site	*n*	*s*	*d*	Fossils
		Dark-Red Medium-Grained Sandstone ($J_{2t}(J_m)$)		
11	12	206	86	*Ginkgoites sibericus*
12	12	260	86	*Baiera cf. gracilis*
13	12	264	88	*Pterophyllum sp.*
14	12	257	78	
15	12	247	77	
		Dark-Red Coarse Medium-Grained Sandstone (J_{3q}-K_{1h} (J_u-K_l))		
01	16	284	50	
02	16	284	50	
03	16	282	58	*Rhinocypris*
04	16	274	43	*Cypridea unicostata Gal.*
19	8	242	75	*Cypridea trita Ljubimova*
20	12	242	73	*Origoiliocypris cirrita Mad.*
21	9	239	75	
22	12	118	76	
23	9	99	74	
24	10	113	56	
25	13	89	66	
28	11	130	26	
29	12	274	28	
30	13	308	18	
31	12	281	26	
32	13	277	24	
33	12	281	27	
		Pale Red Color Fine-Grained Sandstone (K_{2d}-E_{1-2z} (K_u-T_l))		
05	12	86	54	
06	12	93	56	*gastropod bivalve*
07	11	88	56	
08	9	274	98	
09	13	269	97	
10	12	270	50	
16	7	247	77	
17	10	245	79	
18	12	247	75	
26	12	89	64	
27	14	90	68	
34	12	121	30	
35	7	116	30	
36	9	99	32	
37	12	280	105	
38	12	277	100	

Abbreviations are n = number of minicores collected from site; s, d = strike and dip (in degrees) of site beds (dips greater than 90° denote inverted beds; strike is counterclockwise from downward dip). Formation names are J_{2t} = Totuenhe Fm. (middle Jurassic), J_{3q} = Qigou Fm. (late Jurassic), K_{1h} = Hutubi Fm. (early Cretaceous), K_{2d} = Donggou Fm. (late Cretaceous, and E_{1-2z} = Ziniquan Fm. (early Tertiary).

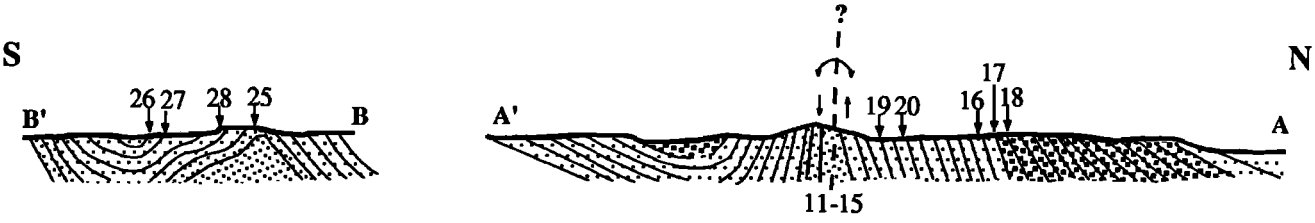

Fig. 3. Schematic N-S cross-sections in eastern part of sampling area (see Figure 2 for location).

The Qigou Formation has yielded ostracodes suggesting a Jurassic age. The Hutubi Formation is reported to contain Early Cretaceous ostracodes such as *Cypridea unicostata Galeeva, C. trita Ljubimova, Rhinocypris echinata Ljubimova* and *Origoiliocypris cirrita Mandelstam.* The latter two species suggest a Barremian age (J. F. Babinot, personal communication, 1989).

Stratigraphically, the Hutubi Formation is part of the Tugulu Group, which according to *Chen* [1983] spans the entire early Cretaceous. The Hutubi Formation is overlain by the Shengjinkou Formation, itself overlain by the Lianmuqin Formation. In Wuerhe district, in the northwestern part of the Dzungar Basin, the Lianmuqin Formation has yielded a fairly varied vertebrate fauna [*Dong*, 1973] containing, among others, the dinosaur Psittacosaurus. Psittacosaurus is known in several other localities in Asia, from Siberia and Mongolia to northern China and Thailand [*Buffetaut et al.*, 1989], in rocks which seem to correspond to the later part of the early Cretaceous (Aptian/Albian). The older Hutubi Formation is thus probably pre-Aptian in age.

The strata outcrop on steeply dipping (>50°) limbs of anticlines with roughly east-west fold axes (Figures. 2 and 3). Altogether, 211 cores were collected from 17 sites. Twelve of the sites are from the northern limbs of the folds (Table 1 and Figure 2).

Late Cretaceous Donggou (K_{2d}) - Early Tertiary Ziniquan (E_1-$_2z$) Formations

The Donggou Formation has yielded ostracodes; its lateral equivalent, the Ailikehu Formation, has also yielded hadrosaurid dinosaurs indicating a late Cretaceous age. These formations are referred to the Maastrichtian by *Chen* [1983] and, to the Coniacian/Santonian by *Hao et al.* [1986]. In the Ziniquan Formation, we have collected gastropods and bivalves of Tertiary aspect (A. Lauriat-Rage, personal communication, 1989). This formation has yielded few fossils. It is referred to the Paleocene/Early Eocene by *Li* [1984].

This strongly folded sequence crops out farthest North of the Tien Shan Mountains. The dips of the strata are generally greater than 50° and are sometimes overturned. The fold axes have orientations similar to those of folds to the south. Sampled rocks are fine-grained sandstones with a pale red color. A total of 174 cores were sampled from 16 sites, 8 of which are on the northern limbs of the anticlines (Figure 3).

PALEOMAGNETIC RESULTS

Minicores were collected with an electrically powered portable drill with standard 2.5-cm-diameter drill bits and were oriented with magnetic and Sun compasses. The average magnetic declination in the region of study is 4°W. In the laboratory the samples were cut into 2.2-cm-long specimens.

Most magnetic measurements were carried out in the magnetically shielded room of the Paleomagnetic Laboratory at the Institut de Physique du Globe de Paris (IPGP), with a three-component cryogenic magnetometer. The remainder of measurements were done at the Paleomagnetic Laboratory of the Université de Rennes (UR), using a single axis cryogenic magnetometer and a Schonstedt spinner flux gate magnetometer. A total of 282 specimens were measured. The intensities of natural remanent magnetization (NRM) ranged from 1 to 200 mA/m, averaging 2 mA/m. Most specimens were thermally demagnetized, in the laboratory-built furnace at the IPGP and in a Schonstedt furnace at the UR, and several specimens were demagnetized by alternating field (af). Thermal demagnetization was found, in general, to be more efficient than af in separating magnetic components. Samples were usually demagnetized over 10 to 16 steps, sample orientation in the furnace being inverted at each step to detect any systematic magnetization resulting from an ambient magnetic field in the furnaces. Demagnetization results were plotted as orthogonal vector diagrams and as equal-area projections. After each temperature step, the bulk susceptibility of each specimen was measured. Curie temperature (CT) analyses in air and isothermal remanent magnetization (IRM) experiments were carried out on about 20 specimens.

Paleomagnetic directions and planes were determined using principal component analysis (PCA; *Kirschvink* [1980]), and site means using McFadden's method [*McFadden and McElhinny*, 1988]. Twenty-eight out of 38 sites provided consistent results, which are described sequentially below.

Middle Jurassic Totuenhe Formation (J_{2t})

Both thermal and af demagnetization methods were used, but thermal demagnetization was much more effective for all five sites (Figures 4*a* versus *b*). In general, vector diagrams from both types of demagnetization demonstrate the presence of two magnetic components with closely aligned directions. The low temperature component (LTC) was cleaned by about 200°C. The Fisher average for this component, based on 20 specimens from the five sites, is Dg=8.3°, Ig=66.9° (k=54.9 and α_{95}=4.2°) in geographic coordinates, i.e., close to the direction of the present Earth's field (PEF) (D=0°, I=62°).

In specimens from site 14, the high temperature component (HTC) is unblocked by about 575°C for the specimens of site 14 (Figure 5*b*); measurements of IRM and Tc on this site (Figures 4*c* and 4*d*) suggest that the remanence is carried by magnetites. For the other sites, the HTC has an unblocking temperature of 620°C suggesting that hematite is a contributing carrier (Figures 4*a* and 5*a*). Measurements of low-field susceptibility do not indicate major changes of magnetic mineralogy during thermal demagnetization (Figure 4*e*). Twenty samples from five sites yielded HTC directions rather close to the PEF in geographic coordinates, though with a slightly steeper inclination: Dg=6.6°, Ig=72.6° (k=107.9 and α_{95}=7.4°). This direction becomes very shallow and mostly upward in stratigraphic coordinates: Ds= 353.9°, Is=-10.1° (k=50.7 and α_{95}=10.8°; see Figures 6*a* and 6*b* and Table 2).

Because this formation is almost monoclinal, no

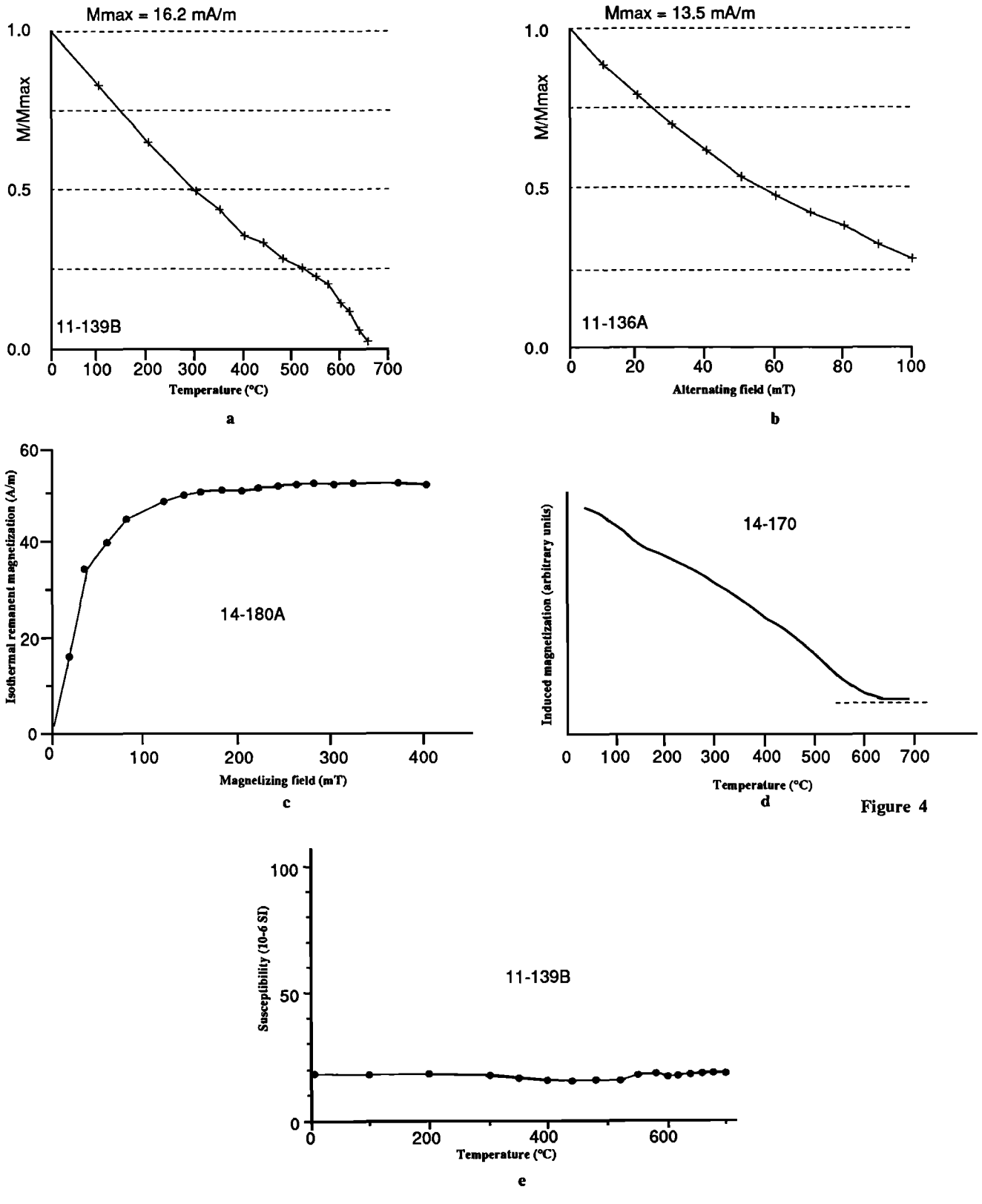

Figure 4

Fig. 4. Results of magnetic study for middle Jurassic (J_{2t}) samples. (*a, b*) Normalized NRM intensity curves showing an unblocking temperature of about 650°C during thermal demagnetization in Figure 4*a*, and a rather high coercivity during af demagnetization in Figure 4*b*. Mmax is the maximum magnetization measured during demagnetization. (*c*) Acquisition of IRM indicating predominant magnetite for site 14. (*d*) Thermomagnetic curve in air showing a decrease of magnetic intensity at about 580°C, also indicative of magnetite for the same site. The applied magnetic field is about 0.5 T. (*e*) Susceptibility curve demonstrating absence of magnetic mineral change during thermal demagnetization.

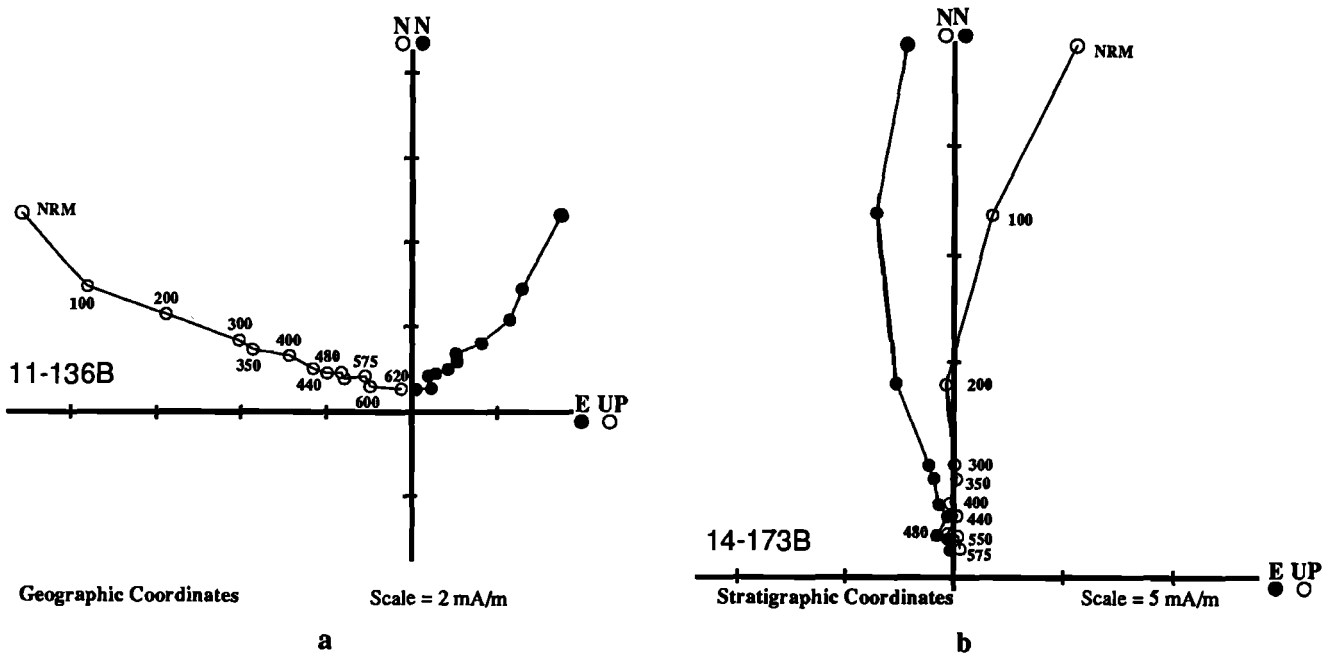

Fig. 5. Orthogonal vector projection of representative thermal demagnetizations from middle Jurassic (J_{2t}) samples demonstrating (1) different unblocking temperatures for different sites; (2) steeper directions than present Earth field (PEF) in (*a*) geographic coordinates and (*b*) horizontal directions in stratigraphic coordinates. Solid symbols are in horizontal plane, and open symbols in NS vertical plane. Numbers adjacent to data points indicate temperatures (degrees Celsius).

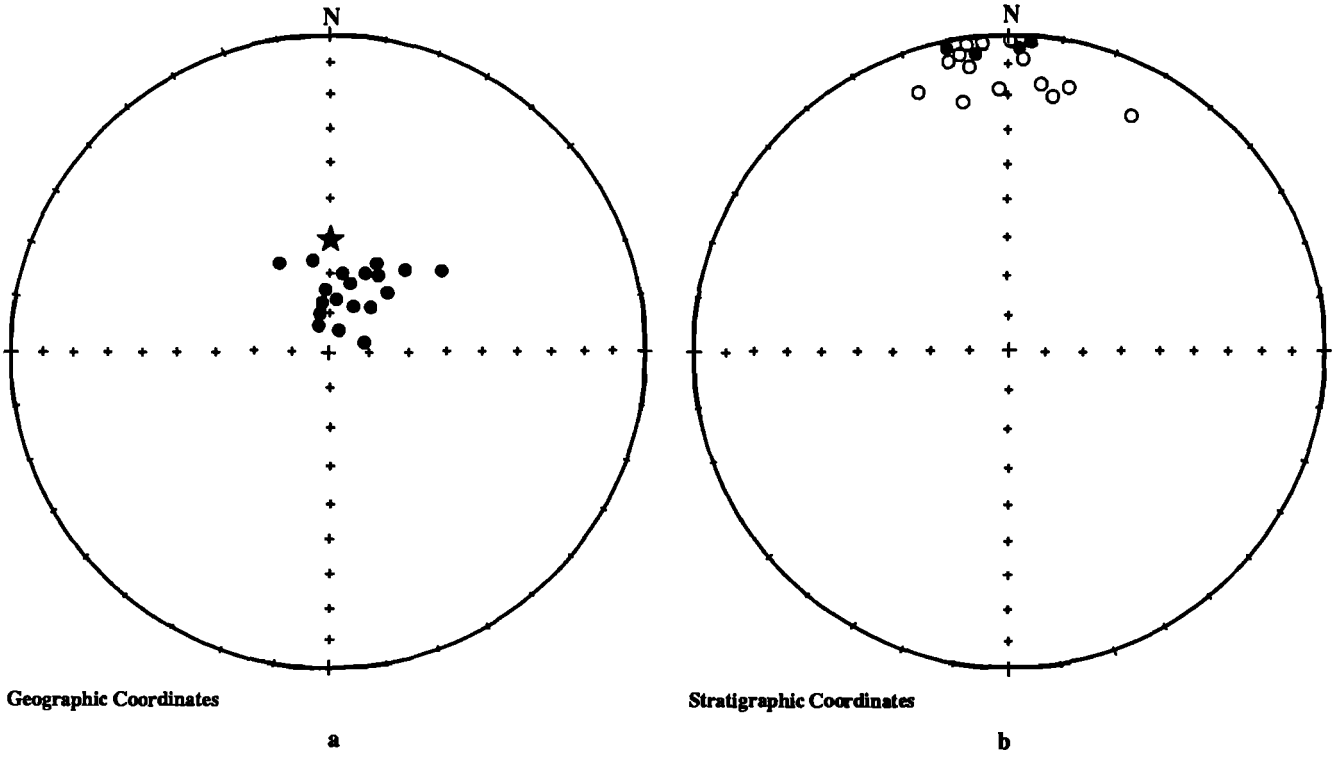

Fig. 6. Equal-area projection of high temperature component (HTC) directions of all middle Jurassic (J_{2t}) specimens (*a*) before and (*b*) after bedding correction. Note that most directions are steeper than present Earth field (PEF, shown by a star) in geographic coordinates and very shallow in stratigraphic coordinates. Closed (open) symbols are for directions in lower (upper) hemisphere.

TABLE 2. Paleomagnetic Directions for J_m Sites

Site	n/N	D_g	I_g	D_s	I_s	k	α_{95}
11	4/4	16.8	69.3	359.0	-17.3	41.5	14.4
12	4/4	346.5	75.4	348.4	-10.6	28.4	17.6
13	4/4	23.6	70.3	4.0	-15.6	36.3	15.5
14	4/4	338.4	68.1	344.1	-10.1	66.1	11.4
15	4/4	28.8	74.2	354.3	3.8	31.8	16.5
Mean	n/N	D_g	I_g	D_s	I_s	k	α_{95}
	5	6.6	72.6	-	-	107.9	7.4
	5	-	-	353.9	-10.1	50.7	10.8

The *n/N* is number of entries in the statistics/number of demagnetized samples;

D, I, k, α_{95} is declination, inclination and *Fisher* [1953] statistics of site-site data. Subscripts *g* and *s* stand for geographic and stratigraphic coordinates, respectively.

significant fold test could be performed, although the best estimate (*k*) of the precision parameter decreases by a factor of 2 upon tilt correction (this is not significant at the 5% level for *N*=5 sites). Also, it is very unlikely that these beds have acquired their magnetization before folding, since this should imply a subequatorial paleolatitude of the area by the middle Jurassic. On the other hand, if the characteristic component corresponds to a remagnetization, it is clear from Figure 6 and Table 2 that its direction is distinct from that of the PEF, but with an inclination intermediate between PEF (*I*=62°) and bedding plane dip (85°N). Two possible causes could account for this observation. Either (1) there is a discrete remagnetization event before the end of folding of the units. In this case, about 10% of partial unfolding would restore HTC directions parallel to PEF; or (2) there is a deviating effect due to a strong anisotropy of magnetic susceptibility (AMS). A few measurements of the AMS of these samples were made on a Digico apparatus [e.g., *Collinson*, 1983] at Rennes University (e.g., see *Cogné* [1988*a*] for the procedure). They show that the AMS ellipsoid is oblate with minimum susceptibility normal to bedding and that the ratios of maximum to minimum susceptibility are rather high, averaging about 1.15. A deviating effect of AMS on magnetization aquisition is thus conceivable, as has already been documented in other examples [*Cogné*, 1988*b*]. With the data presently available, it is not yet possible to conclude which explanation is correct. However, a recent remagnetization event leading to a PEF direction and deviated by the anisotropy is probably a good hypothesis. As mentioned above, the rocks making up this formation are rather coarse and soft, so that the remagnetization was possibly caused by chemical/fluid reactions.

Late Jurassic Qigou (J_{3q}) - Early Cretaceous Hutubi (K_{1t}) Formations

It is clear that thermal demagnetization is much more efficient than af for most specimens (Figures 7*a* and 7*b*). Specimens from this formation exhibit two components of magnetization. The low temperature component (LTC) unblocks by 200° or 300°C. The mean direction of this component is *Dg*=2.8°, *Ig*=62.0° (*k*= 23.6, α_{95}=2.1° and *n*=200) in geographic coordinates, and is not distinguishable from the PEF direction. The *k* value is 10.7 times larger in geographic than in stratigraphic coordinates, clearly indicating a recent overprint. Because the Curie balance experiments were carried out in air, the breakdown of the low temperature part of the thermomagnetic curve in Figure 7*d* is partly due to weight loss. However, the weight loss was measured after the experiments and appeared to be superimposed on a decay of magnetization due either to reaching the Curie point or to the breakdown of a magnetic phase. This suggests the presence of hydroxides such as goethites, and/or sulfides such as pyrrhotites.

As far as the high temperature component (HTC) is concerned, we can divide demagnetization characteristics into three types of behavior. The first type shows magnetizations which cannot be separated from the LTC, close to the PEF (Figure 8*a*). The second type reveals two NRM components; a LTC with unblocking temperature < 300°C and a HTC characteristic component with both normal and reversed polarities (Figures 8*b* and 8*c*). In the third type, demagnetization could not be completed, and the endpoints show only a tendency toward reversed polarity (Figure 8*d*). Comparison of nearby samples with type 2 behavior suggests that the HTC is the same in both types 2 and 3. Hence there is only one characteristic component in these samples. The intersection of great circles, given by the *McFadden and McElhinny* [1988] combined line and plane data analysis method, was used to determine the HTC of type 3 samples, which could then be used in the computation of site mean directions.

The HTCs have unblocking temperatures ranging from 300° to slightly below 600°C (Figure 7*a*), and IRM acquisition curves show that 90% saturation is reached in fields of 150 mT for most specimens (Figure 7*c*). This evidence indicates that the main magnetic carrier is magnetite. However, in some samples, the high temperature part of thermomagnetic curves reveals Curie points above 600°C (Figure 7*d*). This suggests that hematite is sometimes present (e.g., Figures 8*b* to 8*d*) but does not carry a recoverable component of magnetization. No change of bulk susceptibility is found during heating (Figure 7*e*).

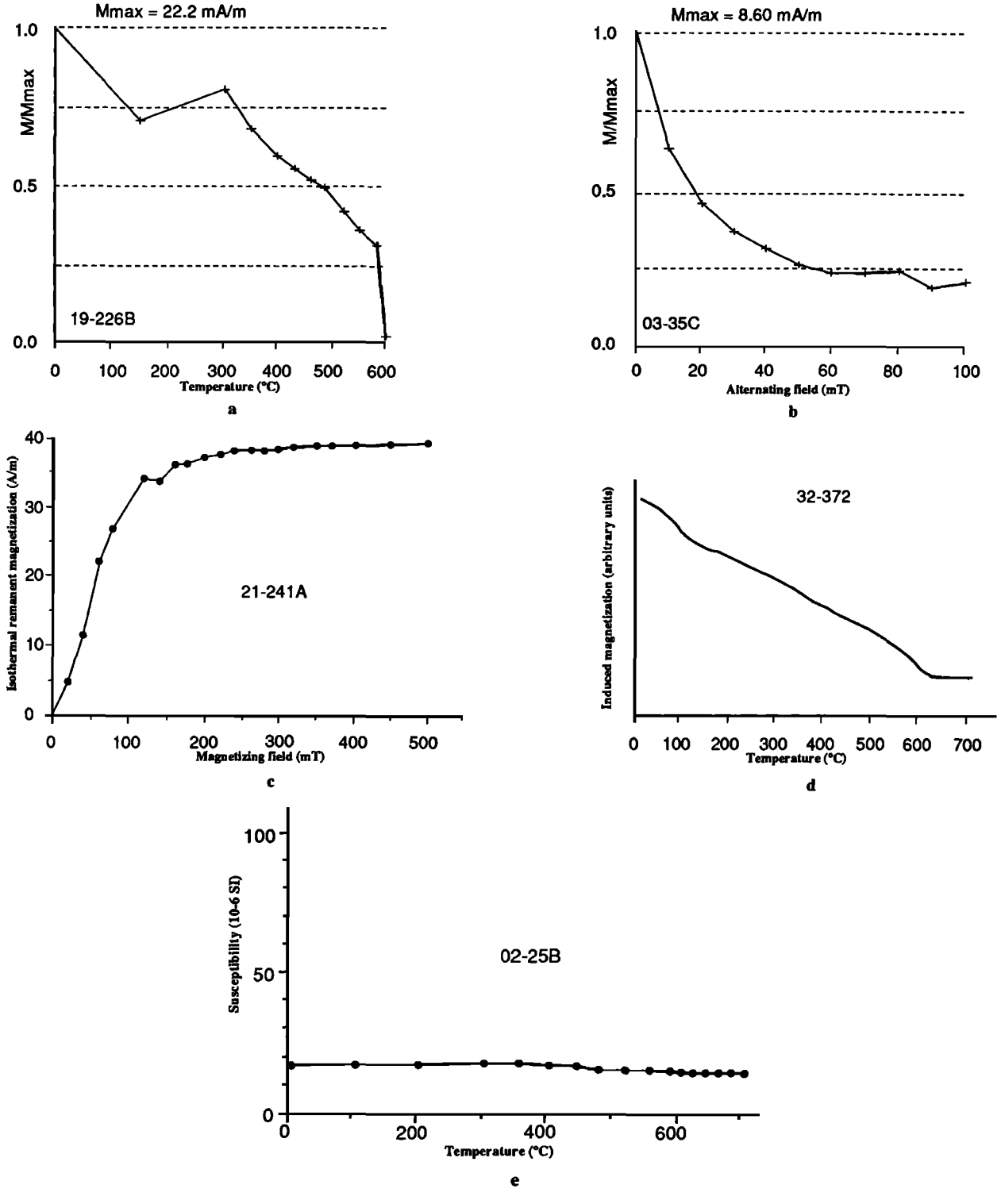

Fig. 7. Results of magnetic study for upper Jurassic-lower Cretaceous (J_{3q}-K_{1t}) samples. (*a*, *b*) Normalized demagnetization intensity curves (as in figures 4*a* and 4*b*, but with unblocking temperature at about 580°C and lower coercivity); (*c*) Acquisition of IRM showing that prominent magnetic carrier is magnetite. (*d*) Thermomagnetic curve in air. Note that Curie points of goethite and magnetite are rather clearly discerned at about 100° and 580°C, together with some hematite with Curie point above 600°C. The applied magnetic field is about 0.6T. (*e*) Susceptibility curve for a representative specimen showing the lack of magnetic mineral change during thermal demagnetization.

From the 17 sites of this formation, four sites were discarded (sites 3, 22, 23 and 24) because of total remagnetization in the PEF direction, or erratic behavior at high demagnetization temperatures (Figure 8*e*). Results from the remaining 13 sites are listed in Table 3. The method of *McFadden and Lowes* [1981] was used to check whether the reversed and normal polarities belong to one direction group. The statistic $p=(R_+ + R_- - R^2/(R_+ + R_-))/2(N - R_+ - R_-)$ (where R, R_+ and R_- are the lengths of the vector sums for the total number of samples (N), normal-polarity samples only (N_+) and

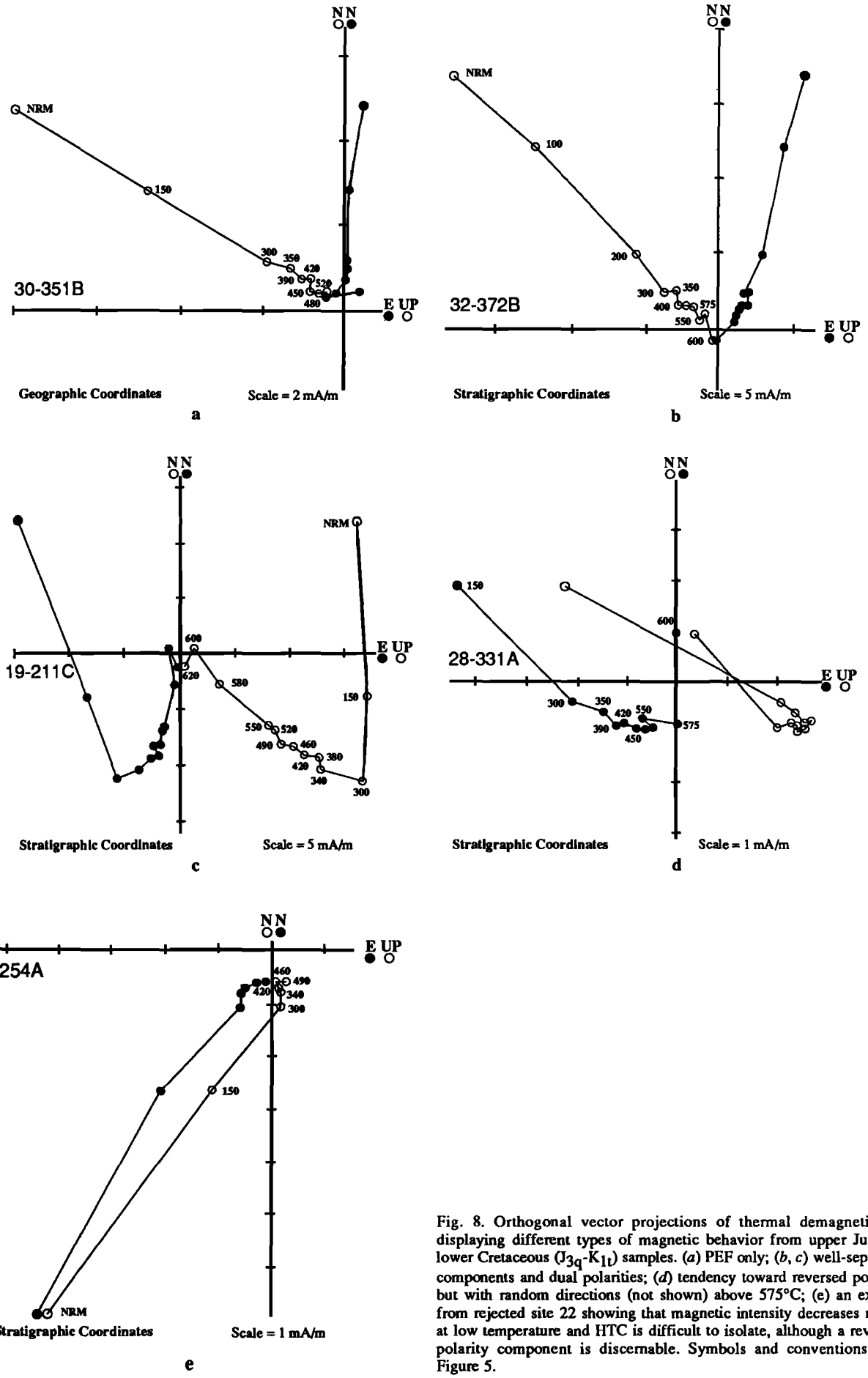

Fig. 8. Orthogonal vector projections of thermal demagnetization displaying different types of magnetic behavior from upper Jurassic-lower Cretaceous (J_{3q}-K_{1l}) samples. (*a*) PEF only; (*b*, *c*) well-separated components and dual polarities; (*d*) tendency toward reversed polarity, but with random directions (not shown) above 575°C; (e) an example from rejected site 22 showing that magnetic intensity decreases rapidly at low temperature and HTC is difficult to isolate, although a reversed-polarity component is discernable. Symbols and conventions as in Figure 5.

TABLE 3. Paleomagnetic Directions for Ju/K_1 sites

Site	n/N	D_g	I_g	D_s	I_s	k	α_{95}				
01	7/9	171.8	77.6	21.5	51.3	15.1	17.8				
02	6/11	33.7	76.4	19.5	42.9	9.9	22.4				
04	7/10	23.2	73.3	10.3	30.5	49.9	8.6				
19	8/8	310.1	-42.0	181.8	-57.1	51.1	7.8				
20	8/9	305.7	-36.6	196.7	-59.6	108.8	5.3				
21	8/8	313.2	-34.4	180.1	-59.3	50.8	8.6				
25	7/8	196.7	20.1	202.0	-42.0	36.7	10.1				
28	8/9	208.5	-22.6	204.1	-47.9	18.2	13.3				
29	6/11	343.6	79.3	355.3	42.7	97.9	9.3				
30	8/11	348.1	66.1	8.0	51.6	118.6	5.1				
31	7/8	50.8	77.7	24.3	53.7	25.1	18.7				
32	8/8	36.9	66.1	23.3	43.8	57.5	8.0				
33	6/8	3.6	68.9	7.4	42.0	34.8	13.1				
Mean	n/N	D_g	I_g	D_s	I_s	k	α_{95}	ks/kg	f(Rg)	f(Rs)	f(Rc)
All	13	55.8	69.2	-	-	4.2	23.0		7.30		0.52
		-	-	12.7	48.6	57.6	5.5	13.7		0.01	
Normal	18	14.3	76.1	-	-	37.7	9.1				
		-	-	11.9	45.5	62.3	7.1				
Reversed	5	365.1	-36.9	-	-	2.2	69.3				
		-	-	194.1	-53.6	61.9	9.8				

Paleolatitude = 26.6° ± 4.8°. Pole: latitude = 72.3°, longitude = 227.3°, A_{95} = 4.8°. The *n/N, D, I, k*, α_{95} are same as in Table 2. The $f(R_g)$ and $f(R_s)$ are computed as $f(R) = (R_s+R_N - R_T2/(R_S+R_N))/2\ (N-R_N-R_S)$, where R_T, R_S and R_N are the length of the vector sums of the site mean directions of all sites (R_T), sites from the southern limbs (R_s) and from the northern limbs (R_N), with $N = N_S + N_N$; $f(Rc)$ is the critical values at the 95% probability level; if $f(R) > f(Rc)$, the hypothesis of a common true mean direction may be rejected [*McFadden and Jones*, 1981].

reversed-polarity samples (N_-), with $N=N_+ + N_-$, respectively) gives 0.028 which is much smaller than the critical values at the 95% probability level, 0.28 (R_- = 4.935, R_+ = 6.917, R = 11.82, N=13). This indicates that the two polarity groups are not significantly different from antipodal.

Only sites 25 and 28 are on the south limb of the fold. However, the stratigraphic correction produces an increase of k from 4.2 to 57.6. The fold test is significant at the 99% confidence level using both the *McElhinny* [1964] and the *McFadden and Jones* [1981] fold tests (Figures 9*a* and 9*b*, Table 3). The mean paleomagnetic direction for this formation is thus Ds=12.7°, Is=48.6° (k= 57.6 and α_{95}=5.5°, in stratigraphic coordinates, Table 3).

Late Cretaceous Donggou (K_2d) - Eocene Ziniquan (E_1-$_2z$) Formations

About half of the samples showed only the PEF or unstable or random directions. The rest (45 out of 102 samples), corresponding to 9 out of 16 sites, yielded two recognizable components. Analysis of IRM and thermomagnetic curves, as well as thermal demagnetizations indicate that LTCs and HTCs correspond to distinct types of magnetic carriers. For LTCs, the unblocking temperature ranges from 100° to 300°C (Figures 11*a* to 11*c*). The low temperature part of the thermomagnetic curves (Figure 10*e*) suggests, as in the previous case, the presence of goethites and/or pyrrhotites. The statistics of this component shows a PEF direction as above. For the HTCs, the unblocking temperatures and magnetic saturations reveal two carriers. One, with a Curie temperature of about 650°C (Figure 10*e*), an unblocking temperature of 650°C (Figure 10*a*) and high coercivity (Figure 10*c*) is probably hematite. The other, which reaches 90% of magnetic saturation at 150 mT (Fig. 10d) and has an unblocking temperature of about 580°C (Figures 10*b* and 11*a*) is probably magnetite.

The behavior of the HTCs is similar to that of the Late Jurassic-Early Cretaceous formations. The sites showing only the PEF direction were eliminated from further analysis. Site-mean directions were computed using the combined line and plane data analysis method of *McFadden and McElhinny* [1988]. No major change of bulk susceptibility was found during heating (Figure 10*f*). Site mean and formation-mean directions are listed in Table 4.

Two of nine sites showed reversed polarities. Comparing the two groups of polarities, the reversal test statistic p is 0.17 (R_+= 6.900, N_+=7, R_-= 1.980, N_-= 2, R=8.860, N= 9). This is smaller than the critical value at the 95% confidence level (0.534), which means that the normal-polarity and reversed-polarity groups are not significantly different from antipodal.

Figures 12*a* and 12*b* show site means with α_{95} confidence limits on equal-area projections before and after stratigraphic corrections. The sites display a large range of structural attitudes. After structural correction, k increases from 2.7 to 56.9. The fold test is positive at the 99% confidence level for both the McElhinny and the McFadden and Jones fold tests (Table 4). The formation mean direction is Ds=12.5°, Is=51.3° (k=56.9 and α_{95}=6.9°, in stratigraphic coordinates, Table 4).

DISCUSSION AND CONCLUSION

A first sampling trip to the Northwestern foot of the Tien Shan, West of Urumqi (44.2°N, 86.0°E), along the southern edge of the Dzungar basin, has provided paleomagnetic results from three age groups. Because age determinations on these continental sediments are unfortunately rather coarse, the

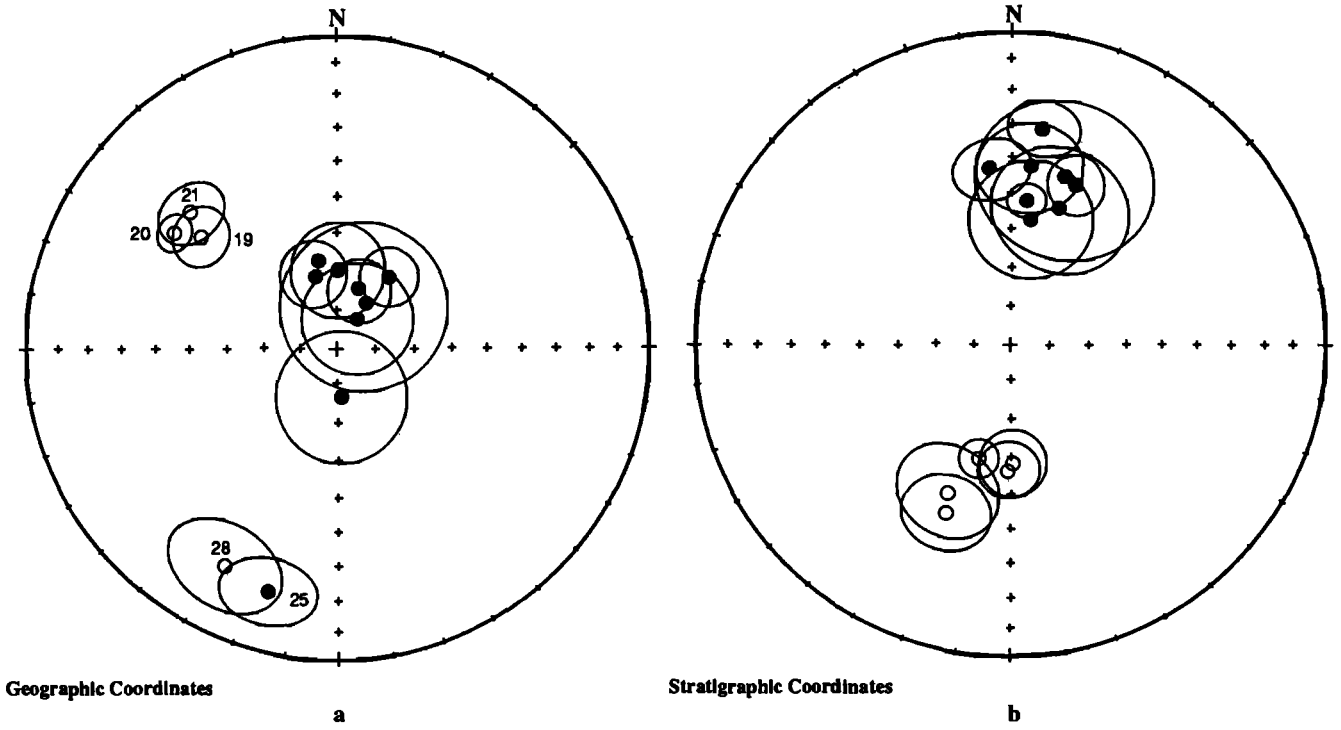

Fig. 9. Equal-area projection of HTC site mean directions from upper Jurassic-lower Cretaceous (J_{3q}-K_{1t}) sites, (*a*) before and (*b*) after bedding correction, with circles of 95% confidence demonstrating positive fold test. Symbols and conventions as in Figure 6.

three age groups cannot be resolved more finely than middle Jurassic, late Jurassic-early Cretaceous, and late Cretaceous-early Tertiary.

Middle Jurassic sites appear to have been completely remagnetized in a direction close to the PEF, after tectonic deformation. It seems particularly difficult to obtain primary paleomagnetic directions from middle Jurassic formations from China, as has been found in South China by *Enkin et al.* [1991b] and M. Steiner et al. (personal communication, 1986). *Courtillot and Besse* [1986] also suggested that lower Jurassic results from both North and South China quoted by *Lin et al.* [1985] might be later remagnetizations.

The late Jurassic-early Cretaceous and the late Cretaceous-early Tertiary age groups yield characteristic paleomagnetic directions which are likely primary with dual polarities and 99% positive fold tests. Even in these formations, about 50% of the samples were remagnetized in the PEF or showed random directions. The Ju-Kl and Ku-Tl poles, based on 13 and 9 sites (with 94 and 45 specimens) respectively, are listed in Tables 3 and 4 and are shown in Figure 13.

It is clear that the two poles (triangle and diamond symbols in Figure 13), which lie within the joint intersection of their α_{95} confidence intervals, are not statistically distinguishable; indeed, their angular distance is 2.3°± 8.0°. Because the magnetizations yielding these two poles predate tectonic deformation, because they have recorded dual polarities and are carried by distinct minerals, they are most likely to be primary, and these two poles can be assigned ages equal to the ages of the formations from which they were obtained.

An implicit assumption in the following discussion is that the recovered paleomagnetic directions are parallel to the geocentric axial dipole (GAD) paleofield direction. Indeed, we must address the question of whether these directions have suffered from compaction-induced inclination shallowing before the paleomagnetic inclinations can be interpreted in terms of paleolatitudes. This problem has recently been analyzed for natural sediments [*Arason and Levi*, 1990*a*], redeposited sediments [*Levi and Banerjee*, 1990], synthetic sediments [*Deamer and Kodama*, 1990] or by numerical modeling [*Arason and Levi*, 1990*b*]. It appears that compaction of magnetite-bearing clay-rich deep-sea sediments may produce a significant inclination shallowing, as high as 15°, especially in the range 45°-60° of initial inclination. However, this phenomenon, which is *not* systematic in deep-sea sediments, is believed to be insignificant, if not absent, in quartz-rich sandstones [*Deamer and Kodama*, 1990; *Stamatakos et al.*, 1989]. Because of the nature of the sediments in our study (coarse-grain continental sandstones), we believe that paleomagnetic inclinations parallel that of the GAD field within the range of experimental error.

The Dzungar Basin was apparently attached to the surrounding blocks (Kazakhstan, Siberia and Tarim) by the upper Jurassic, i.e., the time for which we have our oldest paleomagnetic constraints, with no major tectonic displacements taking place since. We next compare our results with those available for other blocks.

Dzungaria versus Siberia

Paleomagnetic results from Siberia have been obtained by Soviet authors. However, as has been discussed by *Westphal et al.* [1986] and *Besse and Courtillot* [1991], the data reliability is difficult to evaluate. On the other hand, we can follow the assumption of Besse and Courtillot that for the periods of interest here, Siberia was rigidly attached to Eurasia. We can therefore deduce the paleo-positions of Siberia from the apparent polar wander path (APWP) of Europe, where data from Africa, India and North America have been included, based on oceanic reconstructions [*Besse and Courtillot*, 1988, 1991].This APWP is also shown in Figure 13, going back to 200 Ma at 10-Ma intervals.

The data of Figure 13 are plotted in another way in Figure

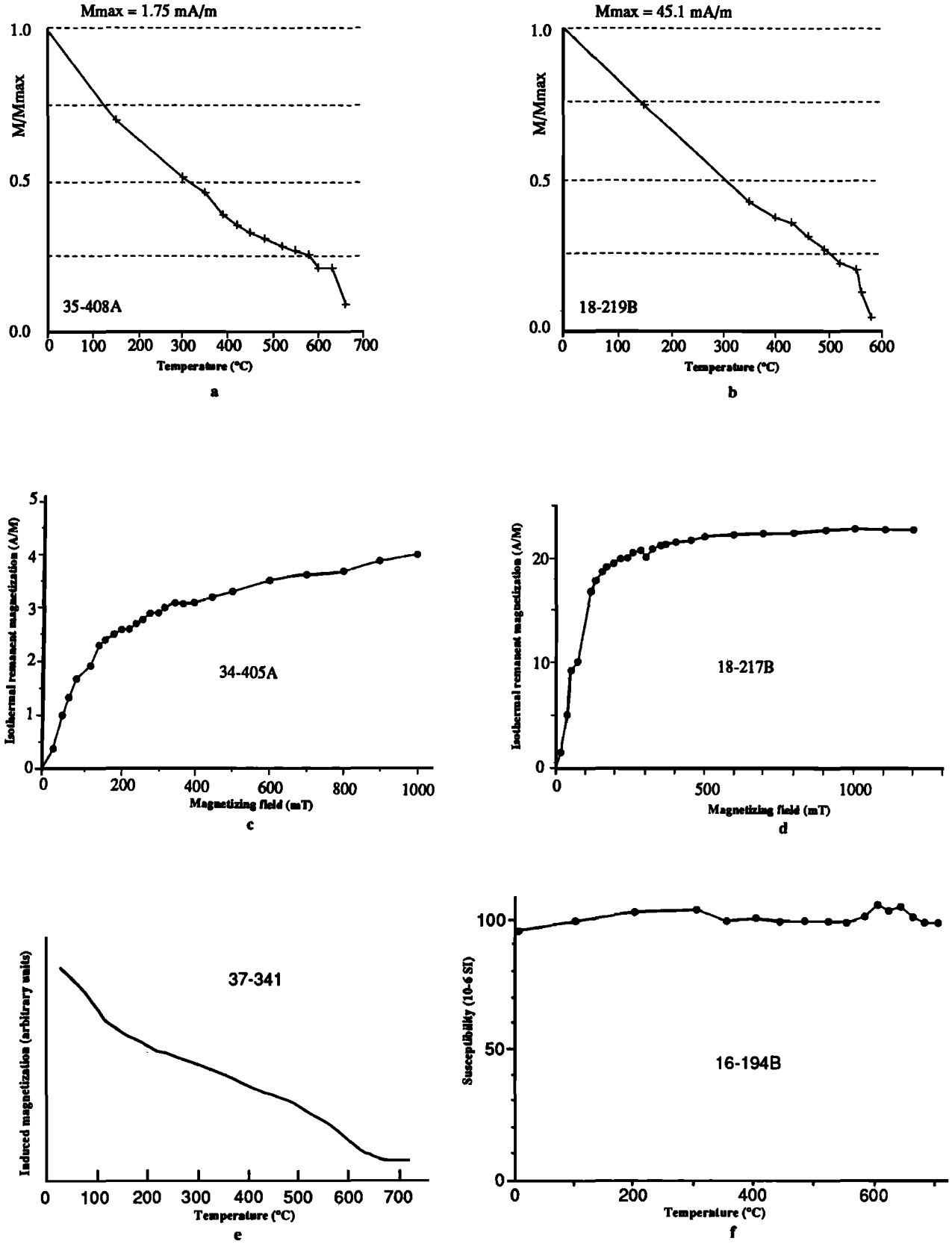

Fig. 10. Results of magnetic study for upper Cretaceous-lower Tertiary (K_{2d}-$E_{1\text{-}2z}$) samples. Normalized demagnetization intensity curves presenting clear unblocking temperatures at about (*a*) 650° and (*b*) 550°C ; IRM acquisition curves for two types of samples, with (*c*) high coercivity minerals (goethite and hematite) and (*d*) a low coercivity mineral (magnetite); (*e*) thermomagnetic curve in air, demonstrating the existence of goethite (about 100°C), hematite (about 650°C) and a fraction of magnetite (580°C), the applied magnetic field is about 0.6T; (*f*) susceptibility curve showing stable susceptibility during thermal demagnetization.

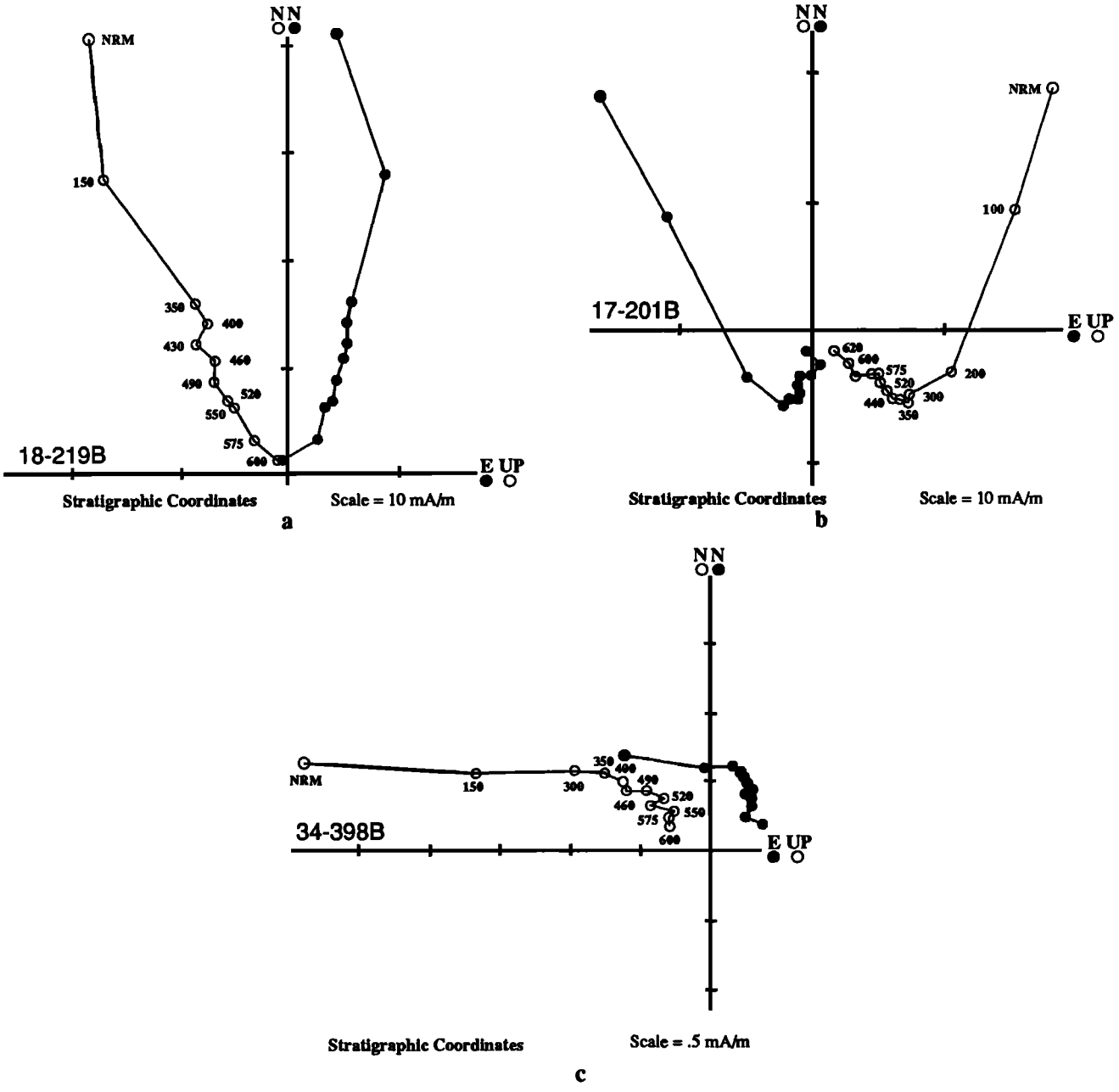

Fig. 11. Orthogonal vector projection of thermal demagnetization from upper Cretaceous-lower Tertiary (K_{2d}-E_{1-2z}) samples, displaying different types of magnetic behavior. (*a*,*b*) Well-separated directions with dual polarity; (*c*) representative of some specimens showing only a tendency toward a final direction. Symbols and conventions as in Figure 5.

14, where the paleolatitudes and declinations obtained for the Dzungar Basin are compared with those deduced from the Besse and Courtillot APWP for a reference site at 44.2°N, 86.0°E. It is clear from Figure 14*b* that at both periods the declinations are virtually identical to those predicted for Eurasia. There is a slightly larger, more systematic difference in terms of paleolatitudes (Figure 14*a*). This difference is smallest, and approximately constant, if the recorded ages of the magnetizations are older than 70 Ma and younger than 130 Ma. Although the ages based on paleontology are allowed to be some 10 Ma younger and older than these values, respectively, this would imply increased paleolatitude differences for which there is no geological evidence: significant convergence and a suturing event in the upper Jurassic (?) on one hand, and divergence and possibly basin opening in the Eocene, i.e., at the time of onset of the India-Asia collision. We assume that samples with ages older than 130 Ma and younger than 70 Ma represent only a small part of our collection and have therefore little influence on the means. The J/K and K/T poles are therefore assigned ages of 130-110 Ma and 90-70 Ma, respectively.

We see in Figure 13 that the K/T pole of the Dzungar block is concordant with 70-90 Ma poles of the Besse and Courtillot APWP, with a large joint intersection of confidence intervals and an angular distance of 6.4°±6.6°. In the 90-70 Ma window, the paleolatitude and declination differences between Eurasia and Dzungaria are not significantly different from zero (5.5°± 6.6°, and 3.4° ± 7.2°, respectively, Figures 14*a* and 14*b*). The J/K pole of the Dzungar block is also close to the 130-110 Ma poles of the Besse and Courtillot APWP (Figure 13), although

TABLE 4. Paleomagnetic Directions for Ku/Tl Sites

Site	n/N	Dg	Ig	Ds	Is	k	α95				
05	5/9	188.7	1.3	195.6	-51.2	19.9	17.6				
10	7/9	42.2	85.3	4.4	37.3	22.8	12.9				
16	6/6	126.5	49.1	8.4	49.3	191.0	4.9				
17	7/8	320.8	-29.1	178.2	-64.7	51.3	8.5				
18	8/8	106.2	46.2	19.3	37.0	28.6	10.5				
26	2/7	2.3	-5.6	5.2	58.3	-	-				
34	4/10	28.9	28.6	27.2	58.5	17.7	22.5				
35	4/9	21.9	17.0	17.8	48.2	9.9	26.9				
36	2/5	11.4	22.2	12.9	54.6	-	-				
Mean	n/N	Dg	Ig	Ds	Is	k	α95	ks/kg	f(Rg)	f(Rs)	f(Rc)
All	9	41.4	41.9	-	-	2.7	39.4		3.91		
		-	-	12.5	51.3	56.9	6.9	21.1		0.19	0.94
Normal	7		43.2	-	-	3.3	49.3				
		36.6	-	13.3	49.3	59.9	7.9				
Reversed	2	-	-31.1	-	-	-	-				
		246.1	-	188.6	-58.2	-	-				

Paleolatitude = 32.0° ± 6.4°, Pole : latitude = 74.3°, longitude = 223.1°, A95 = 6.4°, Legend as in Table 3.

the intersection of confidence intervals is smaller and the angular distance is statistically distinct from zero, at 6.2° ± 5.1°. In the 130-110 Ma window, rather constant and consistent paleolatitude and declination differences of 5.9°±5.2° and 2.5°±5.8°, respectively, are found (Figure 14).

Dzungaria versus Tarim

We next compare our Dzungar results from the northern piedmont of the Tien Shan with those of *Li et al.* [1988a] which were obtained on the southern piedmont of the range, at the northern edge of the Tarim craton (Figures 1 and 16). We note that the upper Cretaceous pole position listed by Li et al. unfortunately contains a misprint, which is carried through their paper. Correct values are listed in Table 5 and displayed in Figures 13 and 15. The two poles of *Li et al.* [1988*a*] are within the joint intersection of their 95% confidence intervals, which are rather large, and therefore not statistically distinct at this probability level. If we compare the Dzungar

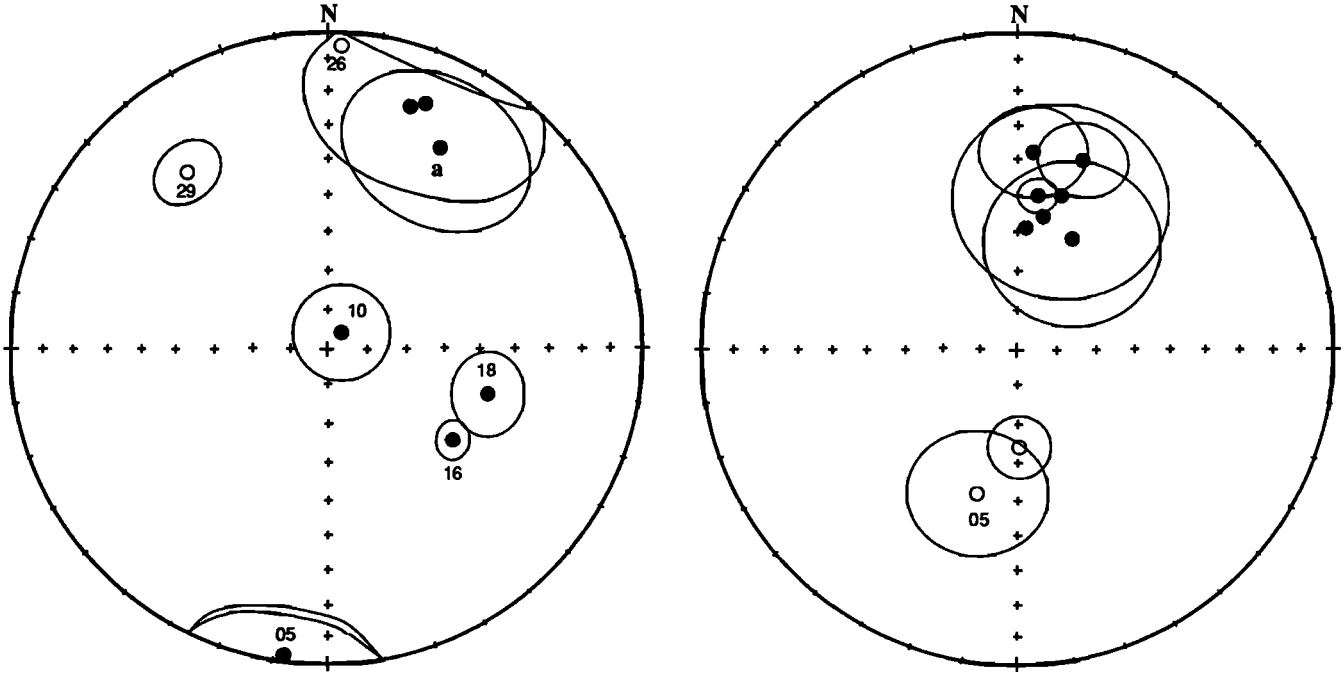

Fig. 12. Equal-area projection of HTC site mean directions from upper Cretaceous-lower Tertiary (K_{2d}-E_{1-2z}) sites, (*a*) before and (*b*) after bedding correction, with circles of 95% confidence demonstrating positive fold test. Symbols and conventions as in Figure. 6.

TABLE 5. Paleomagnetic poles of Tarim, Dzungar and Eurasia

	J/K (130-110 Ma)			K/T (90-70 Ma)		
	λ_p,°N	ϕ_p,°E	$A95$, deg.	λ_p,°N	ϕ_p,°E	$A95$, deg.
Tarim [*Li et al.*, 1988] (recalculated)	64.6	208.4	9.6	66.3	222.9*	8.7
Dzungar (this paper)	72.3	227.3	4.8	74.3	223.1	6.4
Eurasia [*Besse and Courtillot*, 1991]	75.5	207.6	1.9	76.4	199.1	1.8

* The pole longitude, ϕ_p, of the upper Cretaceous Kuche section is misprinted in the paper of *Li et al.* [1988] as 214° both in their Table 2 and in the text, but their global average is correct.

and Tarim poles for the J/K and K/T periods respectively, we find that the Dzungar poles lie barely outside the large uncertainty intervals of the Tarim poles of corresponding age. The angular distances between the pairs of poles are 10.3° ± 10.7° for J/K and 8.0° ±10.8° for K/T (Figure 13). This translates into a Dzungaria versus Tarim paleolatitude difference of 1.9° ± 10.7° and a declination difference of 11.5° ± 11.0° at J/K time, and corresponding values of 6.7° ± 10.8° and 5.2° ± 11.0° at K/T time (Figure 15).

Tectonic Interpretation

The first-order result evident in Figures 13 to 15 is the overall compatibility of the Siberian, Dzungar and Tarim paleomagnetic poles at J/K and K/T times. This is consistent with the proposal that both Tarim and Dzungaria were attached to Kazakhstan and Siberia (and the rest of Eurasia to the north of Cenozoic ranges) prior to upper Jurassic time. The new

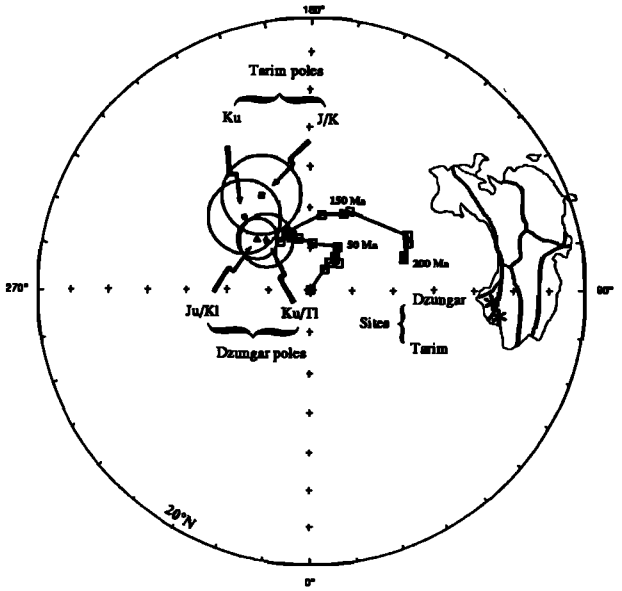

Fig. 13. Apparent polar wander path of Eurasia after *Besse and Courtillot* [1991], marked with open squares connected by a line (time interval between successive poles is 10 Ma). Other poles are solid square = J/K from Tarim [*Li et al.*, 1988*a*], solid circle = Ku from Tarim [*Li et al.*, 1988*a*], triangle = Ju/Kl from Dzungar Basin (this study), diamond = Ku/Tl from Dzungar Basin (this study) and asterisks = Dzungar and Tarim Basin sampling areas.

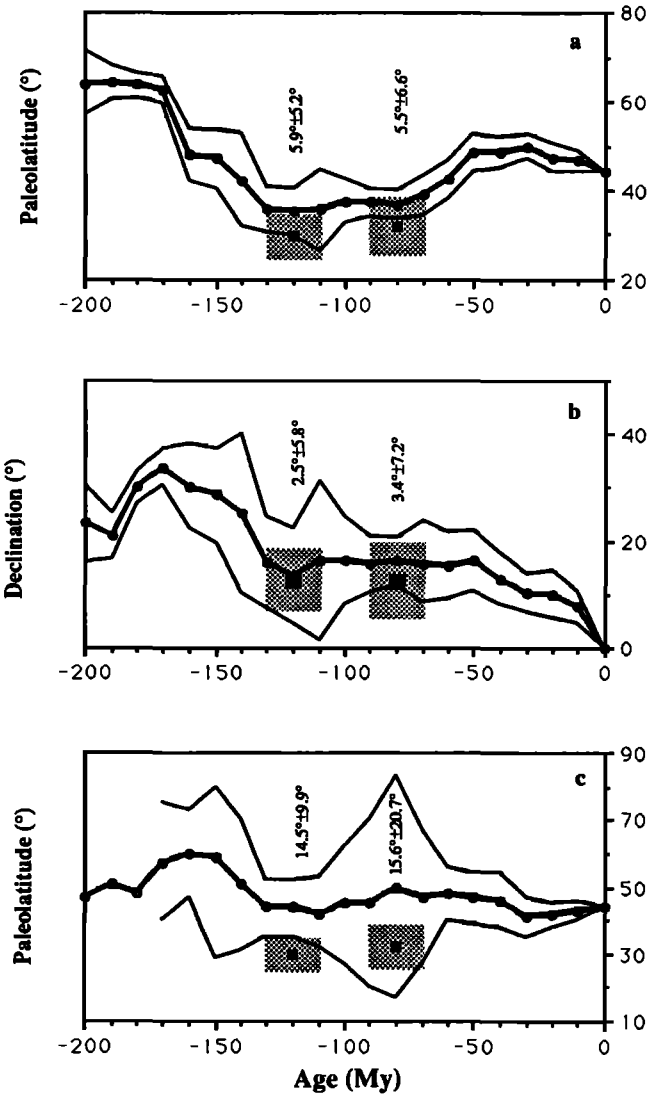

Fig. 14. (*a*,*b*) Predicted paleolatitude and paleodeclination of sampling area calculated from Eurasian APWP of *Besse and Courtillot* [1991]. (*c*) Predicted paleolatitude from *Irving and Irving* [1982] APWP. Squares are results from this study for Ju-Kl and Ku-Tl intervals including error bars on ages and mean directions (stippled areas). Differences between results from this study and reference curves are given.

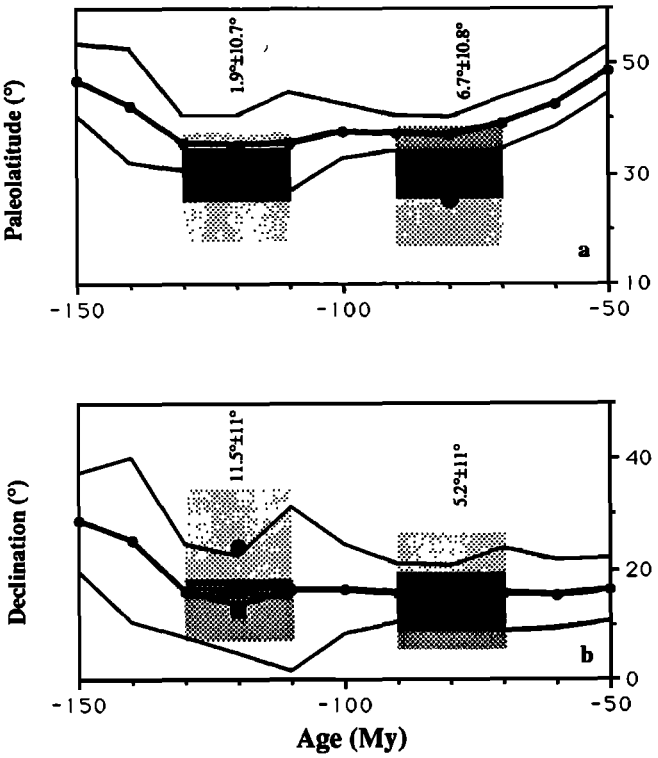

Fig. 15. Detail of (*a*) Figures 14*a* and 14*b*, including results from the Tarim (circles; after *Li et al.* [1988*a*]) and the Dzungar (squares; this study) basins.

poles indirectly lend support to the hairpin loop in the Eurasian APWP at Jurassic and Cretaceous times [*Besse and Courtillot*, 1988, 1991; see also *Enkin et al.*, 1991*a*, *b*). These poles would have been interpreted to indicate large latitudinal displacements, had the *Irving and Irving* [1982] APWP been used. This is clear for instance in Figure 14*c*, where the larger discrepancies and uncertainties in the paleolatitudes are readily apparent. Note that *Li et al.* [1988*a*, p. 219), when discussing *Courtillot and Besse*'s [1986] speculations about differences between the East China and Siberia Cretaceous poles, failed to quote one of their suggestions, namely that the Cretaceous poles of Siberia might be in error. This suggestion has been confirmed subsequently by *Besse and Courtillot* [1988, 1991].

At a finer level of analysis, we note the following observations. The small declination and paleolatitude differences between Dzungaria and Siberia, and between Dzungaria and the Tarim on the other hand, appear to be systematic. These differences can be interpreted in terms of deformation after the deposition age. If we average the K/T and J/K values and correspondingly reduce the uncertainties, we obtain a mean paleolatitude difference of 5.9° ± 3.7° (equivalent to 650 ± 410 km of NS shortening) and a declination difference (or CCW (counterclockwise) rotation) of 2.6° ± 4.5° of Dzungaria with respect to Siberia. In the case of Dzungaria with respect to the Tarim, we find a mean paleolatitude difference of 3.0° ± 6.9° (330 ± 760 km) and a declination difference (CW (clockwise) rotation of Tarim with respect to Dzungaria) of 8.6° ± 8.7°. The large uncertainties on the Tarim poles of course adversely affect these determinations. The values which are significantly different from zero at the 95% confidence level are the shortening between Dzungaria and Siberia, i.e., in the Altai and Sayan Tuva ranges, and (at the edge of significance) the rotation between Dzungaria and the Tarim, i.e., in the Tien Shan.

These values can be understood in terms of a simple model of heterogeneous intracontinental deformation resulting from the India-Asia collision (Figure 16 and J. P. Avouac et al., manuscript in preparation, 1991). It is of interest to examine this deformation in relation to the NNE penetration of India into Eurasia since the Eocene (Figure 16). Although Dzungaria, Kazakhstan and Siberia appear to be parts of the same Eurasian kernel, assembled before the end of the Mesozoic, Dzungaria and Siberia are separated by a major zone of Cenozoic shortening, the Altai and Sayan Tuva ranges. This zone is approximately 700 km wide and 2000 m high on the average, consistent with a 50-km-thick crust, based on isostatic compensation. If this crust had an original thickness of about 35 km, the present thickness implies some 300 km of shortening. This value is likely to be an underestimate, since we have not taken into account additional components of shortening related to (1) the fact that the continental crust in this part of Asia might have been initially thinner, (2) the amount of material removed by erosion, or (3) displaced by lateral extrusion. A total value of about 400 km is possible and compatible with the paleomagnetic estimate of 650 ± 410 km. The Dzungar Basin itself can be approximated by a losange or domino-shaped block, bounded by the overlapping Altai and Tien Shan ranges to the North and South respectively, and by NW to NNW striking right lateral faults (Figure 1). NNE directed shortening should lead to CCW

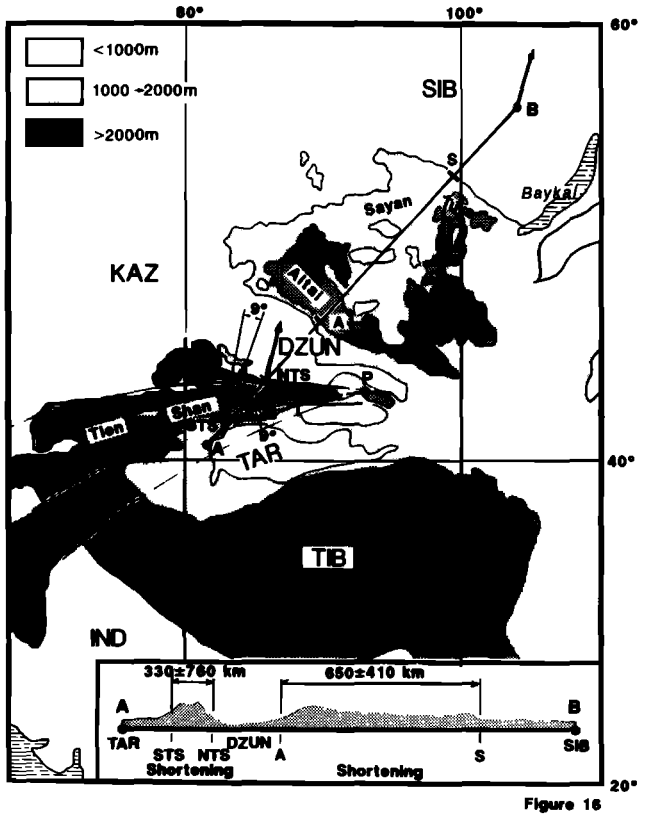

Fig. 16. Schematic topographic map showing major blocks and mountain belts in central Asia, with cross section AB from Tarim to Siberia. Thin great circles crudely outline shape of Tien Shan (J.P. Avouac et al., manuscript in preparation, 1991) and dashed great circle indicates CW rotation of northern edge of Tarim. Arrows show the paleodeclinations of the different blocks. SIB = Siberia, KAZ = Kazakhstan, DZUN = Dzungar, TAR = Tarim, TIB = Tibet, IND = India, STS = southern foot of Tien Shan, NTS = northern foot of Tien Shan, A = southern foot of Altai, S = northern foot of Sayan. Numbers on cross section AB are in kilometers (topography from Simkin et al., [1989] (Mercator projection)).

rotation of the basin [e.g., *Cobbold and Davy*, 1988]. Despite its large uncertainty of 4.5°, the mean rotation which we find (2.6°) is in the correct sense and would correspond to a small amount of additional shortening (20 km).

The Dzungar Basin and the Tarim are separated by the Tien Shan range. This range is very narrow east of Hami, becomes wider to the west and reaches a maximum width of about 400 km north of Kashgar (i.e., some 2000 km to the west), suggesting that the amount of NS convergence increases westward along the range. The wedge shape of the zone of high relief of the range, as defined by its 2000 m altitude contour, may be approximated by two great circles intersecting at a pivot point P some 300 ± 200 km to the East of Urumqi (Figure 16). The mean elevation (about 3000 m) at the longitude of Kashgar implies a crustal thickness of 60 km and some 280 km of shortening with the same simple calculation used above for the Altai. This corresponds to a CW rotation of Tarim with respect to Dzungaria of some 9° about P (the distance between P and Kashgar is about 1800 km, hence 280 km/1800 km = 0.16 rad = 9°, with a combined uncertainty of about 4°). The shortening between our sites in Dzungaria and those of *Li et al.* [1988*a*] in the Tarim is inferred to be of the order of 150-175 km (Figures 15 and 16). Despite large uncertainties which we have stressed above, the orders of magnitude are compatible with the paleomagnetic estimates (9° ± 4° to be compared with 8.6° ± 8.7°, and 150-175 km ± 50% with 330 ± 760 km).

Paleomagnetic constraints now available indirectly for Siberia [*Besse and Courtillot*, 1988] and directly from Dzungaria (this paper) and the Tarim [*Li et al.*, 1988*a*] are thus consistent with the simple model of heterogeneous intracontinental deformation due to the India-Asia collision summarized in Figure 16. The rather large shortening in the Altai range, slight CCW rotation of Dzungaria with respect to Siberia range, increasing shortening in the Tien Shan from East to West and ≈10° CW rotation of its southern piedmont with respect to its northern piedmont, observed or compatible with the paleomagnetic data, are predicted by this model. Note that, as often seems to be the case in paleomagnetism, mean values appear to make more sense than their uncertainties might suggest, leading to the inference that these uncertainties might be overestimated.

The tectonic model embodies the idea that the total amount of shortening between India and Siberia, which is approximately constant in the EW or ESE-WNW direction between 70° and 110°E longitude, is spent in a nonuniform way along the strike of the "overlapping" Tibetan Plateau, Tien Shan and Altai ranges, with recent strain diminishing toward the west in the Altai and Tibet and toward the east in the Tien Shan. The Indian indenter is closest to the Tarim at the longitude of Kashgar. The width of Tibet is minimum there and the northwest tip of India and the Pamirs directly abut the deforming northern boundary of the Tarim, whereas more deformation is absorbed within Tibet to the east. This implies CW rotations of the Tarim and CCW rotation of Dzungaria, which are trapped between the overlapping convergence zones. This means that the Tarim poles of *Li et al.* [1988*a*] and those given here for Dzungaria cannot be considered to be rigidly fixed to either the Siberia block or the North China block. Further work is required to reduce the uncertainties in the Tarim data, to extend the geographical data base for the Tarim and Dzungar blocks and to confirm the preliminary results and interpretation outlined here. Direct Siberian data are also badly needed. Field trips to Siberia, northern Dzungaria and southern Tarim are therefore planned. Until more data become available, the robust conclusion from this study and that of *Li et al.* [1988*a*] is the first-order agreement of Dzungar and Tarim paleomagnetic poles with the *Besse and Courtillot* [1988, 1991] APWP of Eurasia, and the rough agreement of second-order differences with an independently derived tectonic model of heterogeneous deformation in overlapping zones of convergence.

Acknowledgments. R. Butler, N. Opdyke and a third anonymous reviewer made valuable comments on the manuscript. We are also thankful for the suggestions made by R. Enkin. This research has been supported by the Institut National des Sciences de l'Univers and Xinjiang Engineering Institute. This is IPGP contribution 1147.

REFERENCES

Achache, J., V. Courtillot, and Y. X. Zhou, Paleogeographic and tectonic evolution of South Tibet since middle Cretaceous time: New paleomagnetic data and synthesis, *J. Geophys. Res.*, *89*, 10311-10339, 1984.

Arason, P., and S. Levi, Compaction and inclination shallowing in deep-sea sediments from the Pacific Ocean, *J. Geophys. Res.*, *95*, 4501-4510, 1990*a*.

Arason, P., and S. Levi, Models of inclination shallowing during sediment compaction, *J. Geophys. Res.*, *95*, 4481-4500, 1990*b*.

Bai, Y. H., G. L. Cheng, Q. G. Sun, Y. H. Sun, Li Y. H., Y. J. Dong and D. J. Sun, Late Paleozoic polar wander path for the Tarim platform and its tectonic significance, *Tectonophysics*, *139*, 145-153, 1987.

Besse, J., and V. Courtillot, Paleogeographic maps of the continents bordering the Indian Ocean since the Early Jurassic, *J. Geophys. Res.*, *93*, 11,791-11,808, 1988.

Besse, J., and V. Courtillot, Revised and synthetic apparant polar wander paths of the African, Eurasian, North American and Indian Plates, and true polar wander since 200 Ma, *J. Geophys. Res.*, in press, 1991.

Buffetaut, E., N. Sattayarak, and V. Suteethorn, A psittacosaurid dinosaur from the Cretaceous of Thailand and its implications for the palaeogeographical history of Asia, *Terra Nova*, *1*, 370-373, 1989.

Chen, P. J., A survey of the non-marine Cretaceous in China, *Cretaceous Res.*, *4*, 123-143, 1983.

Cobbold, P. R. and P. Davy, Indentation tectonics in nature and experiment, 2, Central Asia, *Bull. Geol. Inst. Univ. Uppsala*, *14*, 143-162, 1988.

Cogné, J. P., Strain, magnetic fabric, and paleomagnetism of the deformed redbeds of the Pont-Réan formation, Brittany, France, *J. Geophys. Res.*, *93*, 13,673-13,687, 1988*a*.

Cogné, J. P., Strain-induced AMS in the granite of Flamanville and its effects upon TRM acquisition, *Geophys. J.*, *92*, 445-453, 1988*b*.

Collinson, D. W., *Methods in Rock Magnetism and Paleomagnetism*, 503 pp., Chapman and Hall, London, 1983.

Courtillot, V., and J. Besse, Mesozoic and Cenozoic evolution of the North and South China blocks, *Nature*, *320*, 86-87, 1986.

Deamer, G. A., and K. P. Kodama, Compaction-induced inclination shallowing in synthetic and natural clay-rich sediments, *J. Geophys. Res.*, *95*, 4511-4530, 1990.

Dong, Z. M., Dinosaurs from Wuerho, *Acad. Sin. Mem. Vert. Palaeontol. and Palaeoanthropol.*, (in Chinese), *11*, 1-7, 1973 .

Enkin, R. J., and V. Courtillot, L. Xing, Z. Zhang, Z. Zhuang, and J. Zhang, The stationary Cretaceous paleomagnetic pole of Sichuan (South China Block), *Tectonics*, in press, 1991*b*.

Enkin, R. J., Y. Chen, V. Courtillot, J. Besse, L. S. Xing, Z. H. Zhang, Z. H. Zhuang and J. X. Zhang, A Cretaceous pole from South China, and the Mesozoic hairpin turn of the Eurasian APWP, *J. Geophys. Res.*, in press, 1991*a*.

Fisher, R. A., Dispersion on a sphere, *Proc. R. Soc. London Ser. A.*, *217*, 295-305, 1953.

Hao, Y. C., D. Y. Su, J. X. Yu, P. X. Li, Y. G. Li, N. W. Wang, H. Qi, S. Z. Guan, H. G. Hu, X. Li, W. B. Yang, L. S. Ye, Z. X. Shou, and Q. B. Zhang, *The Cretaceous System of China*, 301 pp., Geological Publishing House, Beijing, 1986.

Irving, E., and G. A. Irving, Apparent polar wander paths Carboniferous through Cenozoic and the assembly of Gondwana, *Geophys. Surv.*, *5*, 141-188, 1982.

Jaeger, J. J., V. Courtillot, and P. Tapponnier, Paleontological view of the ages of the Deccan Traps, the Cretaceous/Tertiary boundary, and the India-Asia collision, *Geology*, *17*, 316-319, 1989.

Kent, D., G. Xu, K. Huang, W. Zhang, and N. Opdyke, Paleomagnetic

results of upper Cretaceous rocks from south China, *Earth Planet. Sci. Lett.*, *79*, 179-184, 1986.

Kirschvink, J. L., The least-squares line and plane and the analysis of paleomagnetic data, *Geophys. J. R. astron. Soc.*, *62*, 699-718, 1980.

Laveine, J. P., Y. Lemoigne, X. Li, X. Wu, S. Zhang, X, Zhao, W. Zhao, W. Zhu, and J. Zhu, Paleogeography of China in Carboniferous time at the light of paleobotanical data, in comparison with Western Europe Carboniferous assemblages, *C. R. Acad. Sci. Paris*, *304*, 391-394, 1987.

Levi, S., and S. Banerjee, On the origin of inclination shallowing in redeposited sediments, *J. Geophys. Res.*, *95*, 4383-4390, 1990.

Li, C. Y., A preliminary study of plate tectonics of China, (in Chinese), *Bull. Chin. Acad. Geol. Sci.*, *2*(1), 1-19, 1980.

Li, C. Y., Q. Wang, X. Y. Liu, and Y. Q. Tang, *Explanatory Notes to the Tectonic Map of Asia*, 49 pp., The Cartographic Publishing House, Beijing, 1982.

Li, Y. P., R. Sharps, M. McWilliams, A. Nur, Y .A. Li, Q. Li, and W. Zhang, Paleomagnetic results from Late Paleozoic dikes from the northwestern Dzungar Block, northwestern China, *Earth Planet. Sci. Lett.*, *94*, 123-130, 1989.

Li, Y. P., Z. K. Zhang, M. McWilliams, R. Sharps, Y. J. Zhai, Y. A Li, Q. Li, and A. Cox, Mesozoic paleomagnetic results of the Tarim craton: Tertiary relative motion between China and Siberia?, *Geophys. Res. Lett.*, *15*, 217-220, 1988*a*.

Li, Y. P., M. McWilliams, A. Cox, R. Sharps, Y. A. Li, Z. J. Gao, Z. K. Zhang, and Y. J. Zhai, Late Permian paleomagnetic pole from dikes of the Tarim craton, China, *Geology*, *16*, 275-278, 1988*b*.

Li, Y. T., *The Tertiary System of China*, 362 pp., Geological Publishing House, Beijing, 1984.

Lin, J. L., The apparent polar wander paths for the north and south China blocks, Ph.D. thesis, 248 pp., Univ. of California at Santa Barbara, 1984.

Lin, J. L., M. Fuller, and W. Zhang, Preliminary Phanerozoic polar wander paths for the North and South China blocks, *Nature*, *313*, 444-449, 1985.

Mattauer, M., P. H. Matte, J. Malavieille, P. Tapponnier, H. Maluski, X. Z. Qin, L. Y. Lun, and T. Y. Qin, Tectonics of the Qinling Belt: Build up and evolution of eastern Asia, *Nature*, *317*, 496-500, 1985.

McElhinny, M. W., Statistical significance of the fold test in paleomagnetism, *Geophys. J. R. Astron. Soc.*, *8*, 338-340, 1964.

McElhinny, M. W., B. J. J. Embleton, X. H. Ma, and Z. K. Zhang, Fragmentation of Asia in the Permian, *Nature*, *293*, 212-216, 1981.

McFadden, P. L., and D. L. Jones, The fold test in paleomagnetism, *Geophys. J. R. Astron. Soc.*, *67*, 53-58, 1981.

McFadden, P. L., and F. J. Lowes, The discrimination of mean directions drawn from Fisher distributions, *Geophys. J. R. astron. Soc.*, *67*, 19-33, 1981.

McFadden, P. L., and M. W. McElhinny, The combined analysis of remagnetization circles and direct observations in paleomagnetism, *Earth Planet. Sci. Lett.*, *87*, 161-172, 1988.

Molnar, P., and P. Tapponnier, Cenozoic tectonics of Asia: Effects of a continental collision, *Science*, *189*, 419-426, 1975.

Opdyke, N. D., K. Huang, G. Xu, W. Y. Zhang, and D. V. Kent, Paleomagnetic results from the Jurassic of the Yangtze platform, *J. Geophys. Res.*, *91*, 9553-9568, 1986.

Simkin, T., R. I. Tilling, J. N. Taggart, W. J. Jones and, H. Spall, This dynamic planet-World map of volcanoes, earthquakes and plate tectonics, *U. S. Geological Survey*, Washington D. C., 1989.

Stamatakos, J.A., K.P. Kodama, L. Vittorio, and T. L. Pavlis, Paleomagnetism of Cretaceous and Paleocene sedimentary rocks across the Castle Mountain Fault, south central Alaska, in Deep Structure and Past Kinematics of Accreted Terranes, Geophys. Monogr. Ser., vol. 50, edited by J. W. Hillhouse, pp. 151-177, AGU, Washington, D.C., 1989.

Tapponnier, P., and P. Molnar, Active faulting and Cenozoic tectonics of the Tien Shan, Mongolia, and Baykal regions, *J. Geophys Res.*, *84*, 3425-3459, 1979.

Tapponnier, P., G. Peltzer and R. Armijo, On the mechanics of the collision between India and Asia, *Geol. Soc. Spec. Publ.*, *19*, 115-157, 1986.

Wang, S., *The Jurassic System of China*, 350 pp., Geological Publishing House, Beijing, 1985.

Westphal, M., M. L. Bazhenov, J. P. Lauer, D. M. Pechersky, and J. C. Sibuet, Paleomagnetic implications on the evolution of the Tethys belt from the Atlantic Ocean to the Pamirs since the Triassic, *Tectonophysics*, *123*, 37-82, 1986.

Zhang, L. C., and N. Y. Wu, The geotectonic evolution of Tien Shan, *Xinjiang Geol.*, *3*(3) 1-14, 1985.

Zijderveld, J. D. A., A. C. demagnetization of rocks: Analysis of results, in *Methods in Paleomagnetism*, edited by D. W. Collison, K. M. Creer, and S. K. Runcorn, pp. 254-286, Elsevier, New York, 1967.

J.-P. Avouac, Y. Chen, J.-P. Cogné, V. Courtillot, and P. Tapponnier, Institut de Physique du Globe de Paris, Géomagnétisme et Paléomagnétisme (CNRS: UA 729), 4, place Jussieu, 75252 Paris Cedex 05 France.

M. Bai, Bureau of seismology of Xinjiang, People's Republic of China.

E. Buffetaut, CNRS Laboratoire de Paléontologie des Vertébrés, Université Paris VI, France.

M. Li, G. Wang, C. Wei, and H. You, Xinjiang Engineering Institute, People's Republic of China.

(Received April 24, 1990;
revised November 12, 1990;
accepted December 13, 1990.)